Can the Sublimation of Dry Ice Explain the Flattened, Bi-lobate Structure and Spin Rate of 2014 MU_{69}?

AGU100 ADVANCING EARTH AND SPACE SCIENCE

P33I-3541

INTRODUCTION: Part 1

The New Horizons flyby of 2014 MU_{69} (**Arrokoth**) has yielded a wealth of new data on the physical structure and surface chemistry of this small cold classical Kuiper Belt Object (CCKBO). One surprising discovery is the smooth surface of Arrokoth. It shows little sign of impact cratering. This had been predicted by Prentice (2019a). Another discovery is the slow spin rate. This implies that the two lobes of Arrokoth, namely Ultima and Thule, must have given up most of their co-orbital angular momentum if they had formed as independent bodies (Stern et al., 2019).

In this poster I propose that MU_{69} was once the major part of a rapidly spinning, roughly spherical, object of mean diameter ~20 km. If the two lobes of MU_{69} are brought to a common spin axis and we adopt the volumes given in Stern et al. (2019), along with their current spin axis separation distance of 16 km, we obtain a single body spin of ~5.6 hrs. This agrees well with the mean 'single-peaked' period of 5.4 ± 1.6 hrs observed of CCKBOs (Benecchi & Sheppard 2013).

INTRODUCTION: Part 2

I propose that all CCKBOs, including **proto-Arrokoth**, condensed from the outermost gas ring that was shed by the thermally convective protosolar cloud **[PSC]** during its gravitational contraction ~4.6 Gyr ago. The initial size of the **PSC** was ~46.5 AU. The shedding of a discrete system of orbiting gas rings is a key feature of the author's Modern Laplacian Theory of Solar system origin (Prentice 1978, 2015, 2018). The initial mean orbital radius of the CCKBO gas ring was ~36 AU, allowing for the later secular expansion of this orbit due to the loss of mass of the **PSC** though ring shedding. The temperature and mean orbit pressure of that ring are 26.3 K and 1.27 x 10^{-9} bar. The bulk chemical composition of the homogeneous condensate mix is nearly-dry rock (mass fraction 0.5269), graphite (0.0163), H_2O ice (0.1845), CO_2 ice (0.2210) and CH_4 ice (0.0513). The mean density of this mixture at 26.3 K is 1.73 g/cm^3.

A thermal evolution model for **proto-Arrokoth** is constructed assuming that all heat is derived from the decay of ^{26}Al. An initial temperature of 26.3 K is chosen. By time 0.048 Myr, ~50% of the inner CH_4 ice mass has melted and vaporized. It is proposed that although CH_4 vapour rises to the surface, much of it may condense before escaping into space, so forming a solid outer shell of thickness ~0.4 km. At 0.060 Myr, central sublimation of CO_2 ice begins. Within a further 0.016 Myr, all CO_2 ice out to the 0.5 radius point has sublimed. This gas is prevented from escaping because of the outer crystalline CH_4 shell. I conjecture that gas pressure build-up cleaved proto-Arrokoth into two in its equatorial plane. Centrifugal force caused these 'halves' to drift apart until stopped by the drag of ice. This may explain the **flattened, bi-lobate structure of Arrokoth**.

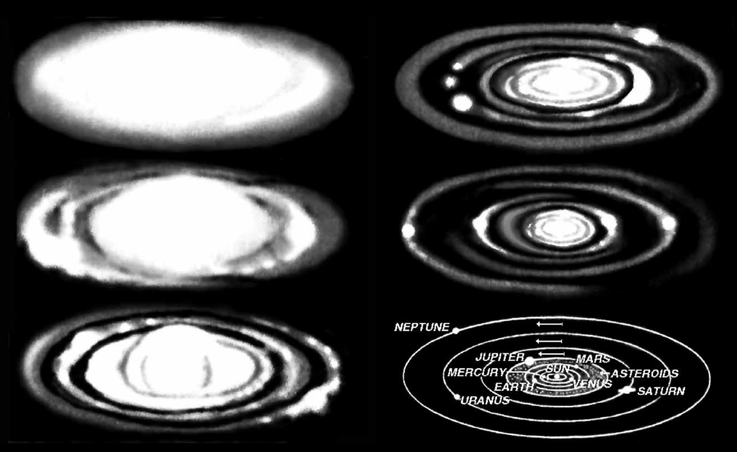

Artist's impression of Laplace's nebula hypothesis. The young, contracting, and rotating proto-solar cloud sheds a system of orbiting gas rings, from which the planets later condense [from drawings by Scriven Bolton, F.R.A.S., Figure 172 of Whipple 1968].

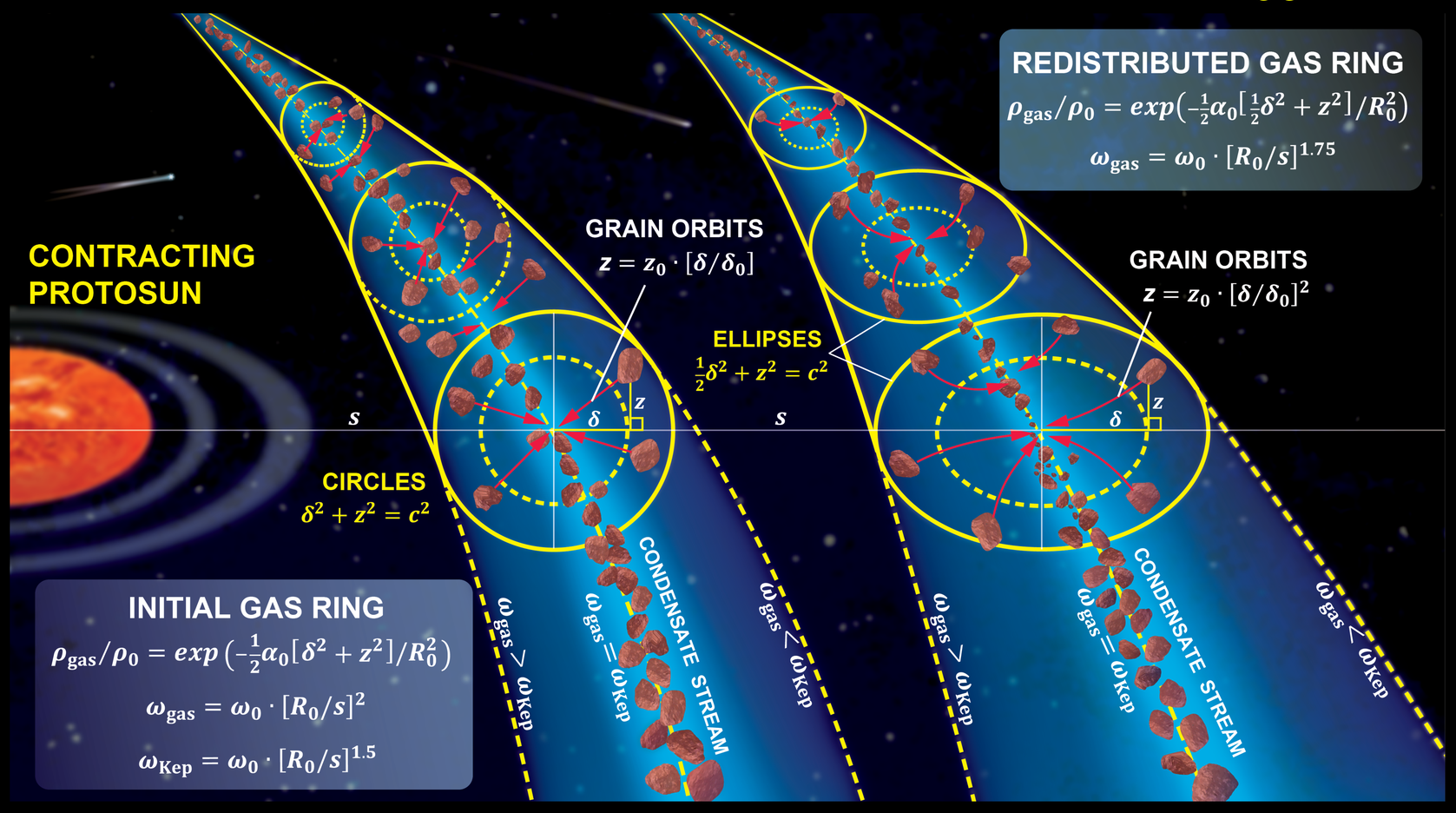

INITIAL GAS RING STRUCTURE AND FOCUSSING OF GRAINS

According to Prentice (1978, 2018), each gas ring has a uniform specific orbital angular momentum $h = \omega_{gas} s^2$. This means that the angular velocity $\omega_{gas} \propto s^{-2}$ declines steeper with increasing cylindrical distance s from the rotational axis of the **PSC** than the local Keplerian angular velocity $\omega_{Kep} = \sqrt{(GM_0/s^3)}$. For illustration, consider the first shed ring (n = 0). Two important results follow:

First, the mass density ρ has a Gaussian-like structure. The density has maximum value $\rho(0)$ on the mean Keplerian orbit {$s = R_0$, z = 0}. It diminishes with the meridional distance $\xi = \sqrt{(\delta^2 + z^2)}$ from the mean orbit according as $\rho(\xi) = \rho(0)\cdot\exp(-0.5\, A\, \xi^2/R_0^2)$. Here $\delta = s - R_0$ is the cylindrical distance from the mean orbit radius R_0 and $A \approx 300$ is a constant.

Second, as soon as a solid grain condenses from the gas it starts to migrate 'spoke-wise' to the central Keplerian orbit of the gas ring, where $\omega_{gas} = \omega_{Kep}$. That is, the gravity of the PSC and the angular velocity distribution of the gas serve to focus all migrating grains onto a single Keplerian orbit in the mid-plane z = 0, to form a concentrated **condensate stream**. This natural focussing property of the gas ring greatly assists the accretion of the condensate grains into larger planetesimals and the subsequent gravitational attraction of these planetesimals to form a single planetary core (cf. Hourigan, 1977). The author's impression of a gas ring and the migration paths of the grains is seen above (see Prentice (2018).

THE MODERN LAPLACIAN THEORY

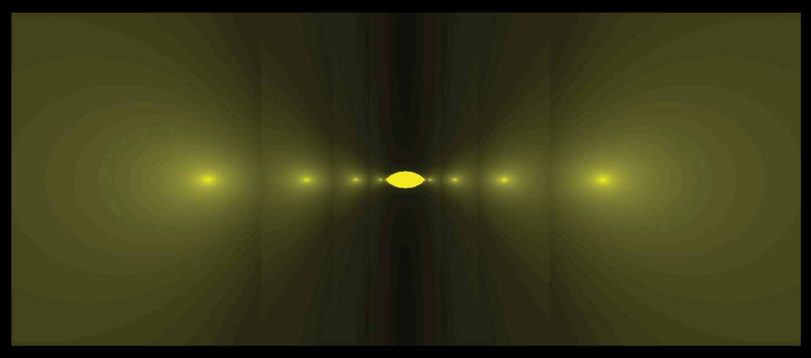

Fully-computational cross-section of the proto-solar cloud (central lenticular structure) and the four outer gas rings shed at the orbits of Saturn through to that of the CCKBOs. Contours show curves of constant mass density. Vertical cylinders define the boundaries between adjacent gas rings.

The author's **'Modern Laplacian Theory [MLT]'** for the formation of the Solar system is a fully quantified reformulation of the original nebular hypothesis due to Laplace (1796). The main assumption of the MLT is that the planetary system condensed from a discrete family of orbiting gas rings. These rings are shed from the equator of the contracting protosolar cloud **[PSC]** as a means for the cloud to rid excess spin angular momentum during gravitational contraction. An artist's impression of the **original Laplace nebula hypothesis** is shown nearby.

If the contraction of the **PSC** takes place uniformly, then both the ratio m_n/M_n of the gas ring mass m_n to the cloud mass M_n, and the axial moment-of-inertia coefficient f_n of the cloud, all stay constant.

The ratio of the mean orbital radii R_n of adjacent of gas rings (n = 0, 1, 2, 3,…) form a **geometric** sequence:

$$\frac{R_n}{R_{n+1}} = \left[1 + \frac{m_{n+1}}{M_{n+1} f_{n+1}}\right]^2 \approx \text{Const.}$$

CHEMICAL CONDENSATION SEQUENCE IN THE GAS RINGS

The most valuable facet of the gas ring model for the formation of the Solar system is its capacity to account for the observed bulk chemical structure of the planetary system. The model predicts a well-defined orbital gradation in the bulk chemical composition of the solid condensate that settles onto the mean orbit R_n of each ring. This gradation comes about as a result of the spatial gradation of the temperature T_n and central pressure p_n of the gas rings, as determined by the thermophysical properties of the protosolar cloud (PSC) at the time t_n of detachment of the ring. The physical and orbital structure of the gas rings ensures that there is **no radial mixing of condensate** between adjacent rings. The chemical mixture of the condensate is thus uniquely determined by its parent ring. The **Table** below gives these quantities for several gas rings, starting with the outermost one (n = 0), corresponding to the orbit R_0 of the CCKBO Quaoar, through to the ring shed at the mean orbit of Mercury (n = 9). The quantities X_{metal}, X_{H2O}, and X_{CO2} are the condensate mass fractions of metal (mostly Fe & Ni) and dry ice. The last column gives the condensate mass density ρ_s. The condensation sequence for the chemical constituents within the system of protosolar gas rings are also given nearby. One diagram is for the **inner system** of protosolar gas rings. The other diagram is for the **outer system** of gas rings. The diagrams show the condensation temperature of $T_{n,j}$ of the individual chemical species { j }. These values are computed for the gas pressure p_n on the mean orbit R_n of each ring. The **heavy yellow curve** defines the blackbody temperature at the equator of the PSC, for a locally detached ring.

THERMOPHYSICAL PROPERTIES OF THE GAS RINGS

The table below gives the basic physical and chemical properties of the gas rings from which each of the listed planets condensed. Because the **PSC** loses mass during contraction, the initial mean orbital radii $R_{n,i}$ of the n^{th} gas ring at the time t_n of detachment from the cloud's equator are smaller than the present values R_n, which are shown. We have $R_n = (M_n/M_{Sun})R_{n,i}$, where M_n is the PSC mass after detachment of the n^{th} ring and M_{Sun} is the solar mass. The pressure on the mean orbit of gas ring is p_n. Also shown are the condensate mass fractions X_j of metal, total water and dry ice. The mean density p_s of the condensate is computed for the present-day orbit temperature.

Planet	R_n (AU)	t_n (10^5 yr)	T_n (K)	p_n (bar)	X_{metal}	X_{H_2O}	X_{CO_2}	ρ_s (g/cm^3)
Mercury	0.387	2.81	1628	0.181	0.7096	0.0000	0.0	5.50
Earth	1.000	2.77	679	4.99×10^{-3}	0.2567	0.0015	0.0	3.80
Ceres	2.767	2.54	272	8.90×10^{-5}	0.0091	0.0418	0.0	3.41
Jupiter	5.203	2.31	158	6.52×10^{-6}	0.0077	0.4900	0.0	1.53
Saturn	9.537	1.99	94	5.39×10^{-7}	0.0084	0.5187	0.0	1.44
Neptune	30.11	0.95	35.5	5.25×10^{-9}	0.0084	0.2421	0.2053	1.76
Quaoar	43.18	0.45	26.3	1.27×10^{-9}	0.0084	0.1858	0.2211	1.80

MONASH University

MoCA Monash Centre for Astrophysics

Andrew J.R. Prentice - School of Physics and Astronomy,
Monash University, Victoria 3800, Australia - andrew.prentice@monash.edu

PROTOSOLAR CLOUD: METHANE–GRAPHITE SYNTHESIS

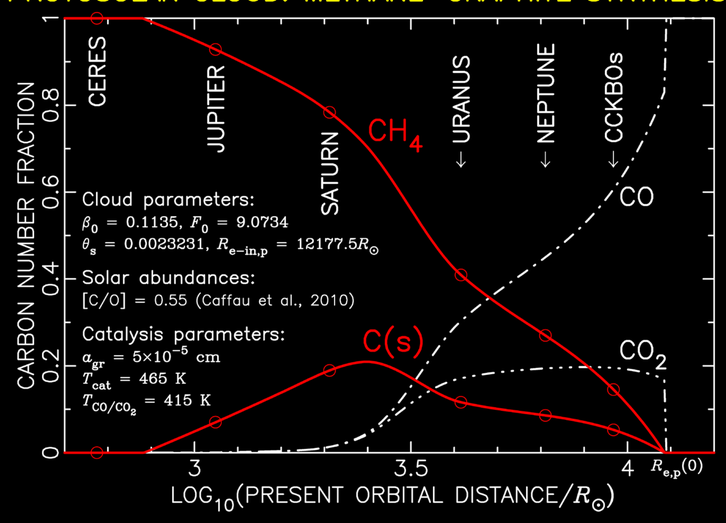

The distribution of carbon number between the four possible states of CO, CO_2, CH_4 and C(s). The carbon numbers have been computed for the gas pressure at the equator of the contracting Protosolar Cloud **(PSC)** and plotted against the present-day equivalent equatorial radius $R_{e,p}$. Initially, all carbon is present as CO. A steady synthesis of CH_4 and graphite C(s) from CO takes place via catalysed reactions on the surfaces of pure metallic grains consisting of Fe, Ni and Co. The CO/CO_2 ratio is controlled by the rapid water-gas shift reaction.

INNER SYSTEM OF PROTOSOLAR GAS

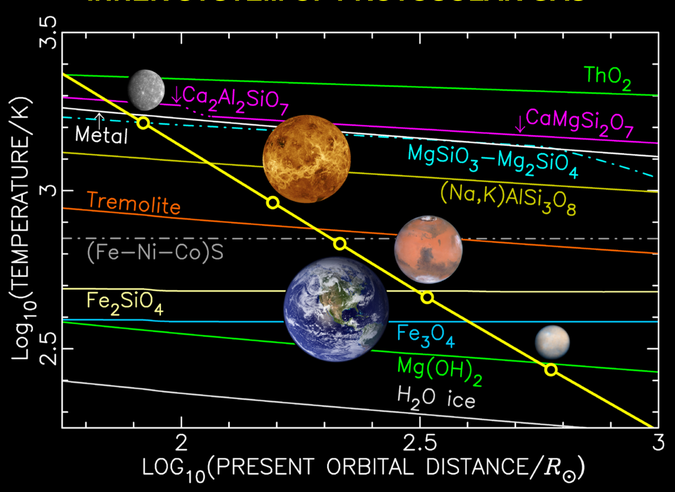

The sequence of condensation temperatures for the principal chemical compounds that form within the five **INNER** gas rings that are shed the contracting protosolar cloud. These temperatures are computed for the gas pressure on the mean orbit of each ring. It is assumed that a gas ring is shed at orbits corresponding to the four terrestrial planets and Ceres.

OUTER SYSTEM OF PROTOSOLAR GAS RINGS

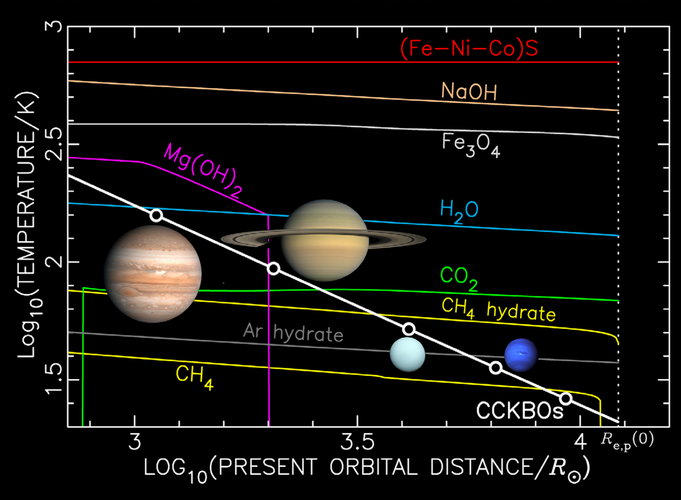

The sequence of condensation temperatures for the principal chemical compounds that form within the five **OUTER** gas rings that are shed the contracting protosolar cloud. These temperatures are computed for the gas pressure on the mean orbit of each ring. It is assumed that a gas ring is shed at orbits corresponding to the four major planets Jupiter, Saturn, Uranus and Neptune and at the mean orbital radius of the large cold classical Kuiper Belt object Quaoar, namely 43.18 AU. It is only at the orbit of the **CCKBOs** that pure CH_4 ice can condense. This was first shown empirically by Prentice (1991), following the homogeneous condensation model of Lewis (1972). It agrees with the conclusion of Doressoundiram et al. 2008).

ACKNOWLEDGEMENTS

The author thanks S. Morton, N. Porcellato and A. Craig for providing much assistance and technical support in producing the graphics in this paper. He thanks P. Cally, J. Cashion, D. Collins, D. Cruikshank, M. Marshall and C. Morgan for helpful discussions. He gratefully also acknowledges the support of the Monash University IT department, especially that of A. Thorne and S. Ziemer.

THERMAL EVOLUTION MODELS FOR PROTO-ARROKOTH

Consider now the thermal evolution of **Proto-Arrokoth**. It is assumed that the initial object is chemically uniform and has the same bulk composition as given by the condensation model.
All heat is assumed to derive from the radioactive decay of ^{26}Al. The specific isotopic heat production rate is 0.4554 W/kg.
The melting and vaporization temperatures of CH_4 and H_2O ice and the sublimation temperature of CO_2 ice are computed at each internal radius point. The initial radius of Proto-Arrokoth is chosen to yield a final radius of **10.0 km** after account is made the loss of CO_2 though sublimation. Further details of the construction of the models are given in Prentice (2019b).
Two models have been constructed. The **first** model was made prior to the flyby of Arrokoth by *New Horizons*. It computes the thermal evolution of Ultima, assuming that this body formed independently of Thule. The model ignores the **latent heat** lost due to phase changes. As a result the mass fractions of melted CH_4 and H_2O ices and that of sublimed CO_2 ice are less than those implied by the thermal profiles in the diagram. The initial chosen radius of 10.5 km is thus too high as it supposes a ~60% loss of CO_2.

ULTIMA THULE SINGLE–LOBE THERMAL EVOLUTION

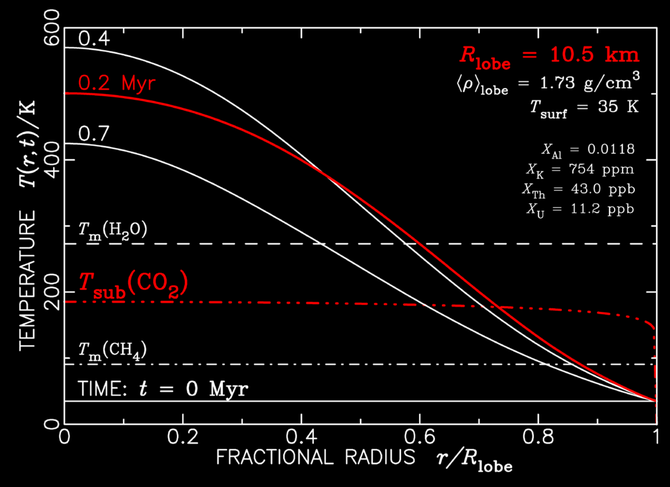

THERMAL EVOLUTION MODELS (continued)

The **second thermal evolution model** assumes that both lobes of Arrokoth, **Ultima** and **Thule**, were once part of single object: **Proto-Arrokoth**. The initial radius of the model, namely R_{obj} = **10.2 km**, is chosen to allow for an eventual loss of mass of ~29% of the initial store of CO_2 due to sublimation. The surface temperature of 26.3 K is that of the condensate from which Proto-Arrokoth (and all CCKBOs) accreted. Consider now the evolution of the individual ices.
CH_4 ice: Vaporization of this ice at the object's centre, where the pressure is 0.44 bars, takes place at time 0.014 Myr after the start of the thermal evolution. By time t = 0.018 Myr, ~30% of the total CH_4 mass has vaporized. After 0.094 Myr, the vapour front has reached the 0.835 fractional radius point, meaning that ~58% of all CH_4 has turned to vapour. All of this vapour is assumed to rise to the surface though porous voids. I now propose that as this vapour passes up though the cold upper layers of Proto-Arrokoth, much of it condenses first to liquid and then to **crystalline ice**.
The thickness of this outer shell is ~360 m.
CO_2 ice: Central sublimation occurs at time t = 0.06 Myr. By time 0.13 Myr, ~20% of the CO_2 mass has sublimed. At time t = 0.028 Myr, the sublimation front has reached it maximum extent, with ~29% of the CO_2 having sublimated. The trapping of the rising CO_2 vapour underneath the outer shell of crystalline CH_4 ice may result in the explosive disruption of the outer shell and destruction of the assumed originally cratered surface of Proto-Arrokoth. As a result, Prentice(2019a) predicted that New Horizons would discover the surface of Arrokoth to be '**globally smooth and crater free**'.
If 90% of the CO_2 vapour escapes into space and the rest is trapped as ice in the outer fractured CH_4 shell, the radius of Proto-Arrokoth shrinks to **10.00 km**. The thickness of the outer frozen CH_4-CO_2 ice increases to 385 m, for mean density of 0.6 g/cm^3, for surface temperature 26.3 K.
H_2O ice: Vaporization at the centre occurs at time t = 0.31 Myr. By time t = 0.43 Myr, the vaporized mass achieves its maximum value of **1.0%**. I assume that this vapour becomes easily frozen and trapped in the outer CH_4-CO_2 shell.

OBJECT PROTO–ARROKOTH THERMAL EVOLUTION

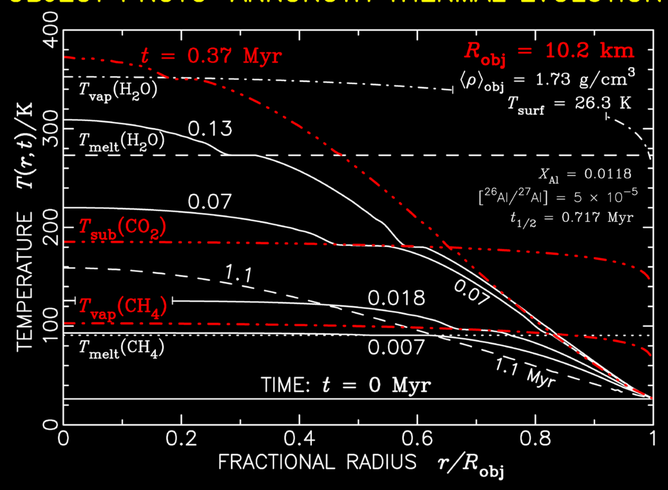

PROTO-ARROKOTH STRUCTURE

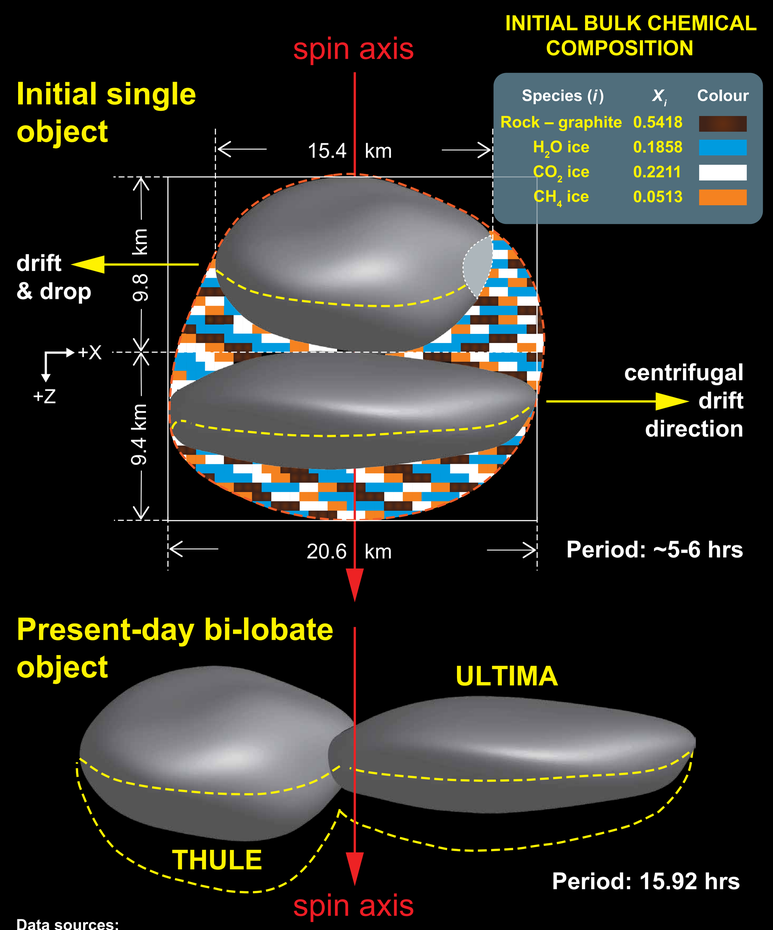

Data sources:
Stern et al. (2019) Science 364, 649
White et al. (2019) AGU Fall Meeting, abstract id. P42C-01
https://www.nasa.gov/feature/new-horizons-evocative-farewell-glance-at-ultima-thule

FORMATION OF ARROKOTH FROM PROTO-ARROKOTH

The underlying assumption of the present study is that the two lobes of MU_{69}, namely Ultima and Thule, were once part of a single rapidly spinning object: **Proto-Arrokoth**. As noted in the **INTRODUCTION**, if the lobes are brought together to a single co-axial body, with Thule stacked on top of Ultima as illustrated in the upper section of the schematic, the resulting single object has a spin period of ~5.6 hours. I adopt the lobe physical dimensions given by White et al. (2019). If we allow for the uncertainty in the data, the spin period is ~5-6 hours. The greatest uncertainty in determining the initial shape of Proto-Arrokoth **(P-A)** is the vertical depth of Ultima. The shaded grey areas are the shapes given by Stern et al. (2019) and the NASA New Horizons news release dated Feb. 9th.
Consider now the **PROTO-ARROKOTH STRUCTURE** schematic. The (x,z)-cross-section of **P-A** is filled both by the grey-shaded NASA sections and by a network of small rectangular tiles. The combination of the tiles is in proportion by area to the mass fractions of the initial condensate mix. This mix is given in the embedded table. The tiled crescent area below Ultima fills in the missing area section indicated by the new 9.4 km depth measurement of White et al. (2019).
In the beginning, before the ^{26}Al decay-driven thermal evolution of **P-A** began, the object was chemically-uniform. All of the area within the outer dashed line boundary was thus 'colour tiled'. Thermal modelling of **P-A** suggests that an outer shell of frozen CH_4 soon forms as a result of early internal vaporization. This event is followed by the **sublimation of CO_2 ice**. If the escape of CO_2 gas is prevented by the impervious nature of the outer CH_4 shell, then disruption of the shell is inevitable. Now because **P-A** is spinning, the equatorial plane is the plane of least net inward load (gravity less centrifugal) due to overlying material. It is thus the plane of easiest escape. I therefore suggest that the escape of CO_2 vapour occurs preferentially in that plane and that, as a result of pressurization due to vapour build up, that **P-A** is roughly cleaved in half in its equatorial plane. The two '**halves**' then drift apart under the action of centrifugal force, riding initially on a cushion of gas.
It is supposed that their drifting apart is stopped by the frictional rubbing action of the gas-free, contact surfaces of each 'half'.

CONCLUSION: The above picture for the formation of the two lobes of Arrokoth is by no means physically complete. Nonetheless, the model presented here does at least show a promising way forward to explain the flattened, bi-lobate structure and the slow spin rate of this remarkable object.

REFERENCES

Benecchi, S. and Sheppard, S., 2013, *Astron. J.* **145**, 124.
Doressoundiram et al., 2008, The Solar System Beyond Neptune', eds. M.A. Barucci et al., (UA Press), p.91.
Hourigan, K., 1977, *Proc. Astron. Soc. Australia*, **3**, 169.
Laplace, P.S. de, 1796, Exposition du Système du Monde (Paris: Courcier).
Lewis, J.S., 1972, *Earth Planet Sci. Letts.*, **15**, 286.
Prentice, A.J.R., 1978, *Moon & Planets*, **19**, 341.
Prentice, A.J.R., 1991, in The Role of Mathematics in Science: a Symposium held at the 1990 Annual General Meeting of the Australian Academy of Science, April 1990, pp. 23-45.
Prentice, A.J.R., 2015, 46th LPSC, abstract id. #2664; 2018, AAS DPS Meeting #50, id.113.03.
Prentice, A.J.R., 2019a, 233rd AAS Meeting, id. 467.01; 2019b, eprint arXiv:1901.02850
Stern, S.A. et al., 2019, *Science* **364**, eaaw9771.
White, O. et al., 2019, AGU Fall Meeting, abstract id. P42C-01.